

Highly efficient channeling of single photons into guided modes of optical nanocapillary fibers

Bashaiah Elaganuru¹, Resmi M¹, Ramachandrarao Yalla^{1*}

¹School of Physics, University of Hyderabad, Hyderabad, 500046, Telangana, India.

*Corresponding author(s). E-mail(s): rrysp@uohyd.ac.in;
Contributing authors: 18phph19@uohyd.ac.in; 19phph18@uohyd.ac.in;

Abstract

We report numerically the efficient channeling of single photons from a single quantum emitter into guided modes of optical nanocapillary fibers (NCFs). The NCF is formed of a liquid core optical nanofiber with inner and outer diameters. We optimize the inner and outer diameters of the NCF filled with water medium by placing a single dipole source (SDS) inside. The maximum channeling efficiency of **52%** is found when the radially polarized SDS is placed at the center of the NCF filled with the water medium. The optimum inner and outer diameters of the NCF are **100 nm** and **360 nm** for the emission wavelength of **620 nm**, respectively. Additionally, we investigate the SDS position dependence inside the NCF considering experimental ambiguity in placing a single quantum emitter inside the NCF. We found that the channeling efficiency remains almost constant for the water medium at the optimum condition. The present platform may open a novel route for generating single photons in quantum technologies and detecting single cells in bio-sensing.

Keywords: Optical nanofibers, Nanocapillary fibers, Single dipole source, Single photons

1 Introduction

In quantum information processing and communication, single photons are employed as information carriers as they are the ideal choice. A quantum network consists of quantum nodes for storing single photons and quantum channels for single photon transmission. Single-mode optical fibers can serve as quantum channels and single

quantum emitters as quantum nodes in a physical implementation of a quantum network. Therefore, efficient channeling of single photons into a single-mode optical fiber is necessary. The generation of single photons nowadays is achieved using various protocols based on single atoms [1], single ions [2], single molecules [3], single quantum dots [4], single vacancy centers in nano-diamonds [5], single defect in silicon carbide [6], rare-earth-ion impurities in yttrium aluminum garnet/yttrium orthosilicate [6], and two-dimensional materials [6].

However, the production of single photons is useless without an efficient manipulation and control manner. Efficiently channeling single photons from a single quantum emitter into a particular mode is a challenging task [7, 8]. Various protocols have been proposed and developed for efficiently collecting single photons. Examples include micropillar cavities [9], solid immersion lens [10], photonic crystal cavities [11], diamond waveguides [12], plasmonic metal nanowires [13], optical nanofibers (ONFs) [14–24], and optical nanofiber tips (ONFTs) [20, 25, 26]. Other than ONF/ONFT, the subsequent coupling of fluorescence photons into a single-mode fiber reduces the actual collection efficiency due to the mode mismatch. Regarding atoms and ions, it is possible to efficiently control the production of single photons on demand. However, it requires complicated experimental setups and intermittent loading of atoms or ions. Regarding solid-state quantum emitters, spectral diffusion and other broadening result in photon distinguishability from the same quantum emitter/various emitters. Collecting single photons from quantum emitters in the high refractive index host materials is challenging.

In addition to efficient manipulation, efficient transmission lines between quantum nodes are also essential for applications in quantum technologies. In such an application, efficient channeling of single photons into single-mode optical fibers (SMFs), playing the role of transmission lines, is required. To achieve this, nanostructured systems have been proposed and demonstrated, including sub-wavelength diameter silica fibers termed ONFs and ONFTs [15–21]. Moreover, for application in quantum network [7], in-line method i.e. fiber integrated light-matter interfaces such as those realized by ONFs/ONFTs are advantageous since automatic channeling to the SMF was achieved [16–19]. However, in these efforts, a maximum channeling efficiency (η) was achieved up to 28% for the radially polarized single dipole source (SDS) [18, 19]. The maximum η -value up to 20% has been experimentally demonstrated for single photons from a single quantum dot directly into the SMF considering randomly oriented dipole [16]. Note that the single quantum dot was placed on the surface of the ONF. It has been numerically shown that a maximum η -value of 38% from the radially polarized SDS to the SMF was achieved using the ONFT [20, 25]. Note that the SDS was placed on the facet of the tip. The feasibility of the simulation results has been experimentally shown by placing quantum dots on the facet of the ONFT [27]. Note that the interaction strength has been limited due to the positioning of the SDS on the surface of the ONF/ONFT.

One can enhance the η -value in two ways: one is creating a cavity on the ONF and the other is placing the single quantum emitter inside the ONF. Regarding the

cavity on the ONF, the maximum η -value of 65% has been experimentally demonstrated using a composite photonic crystal cavity on the ONF [28]. Note that a single quantum dot was placed on the surface of the ONF only, which limits the interaction. Regarding placing the single quantum emitter inside, a new type of hollow core fiber with sub-micron diameter termed as capillary fibers has been proposed and experimentally demonstrated [29]. However, these efforts demonstrated the η -value up to 18% only. This is due to the thicker outer diameter of the capillary fiber, leading to weak confinement of the field inside the capillary fiber. The systematic study of η -value for the hollow/liquid core ONF with inner and outer diameters termed optical nanocapillary fibers (NCFs) has not been reported yet. Note that the inner and outer diameters of the NCF are in sub-wavelength. The position dependence of the SDS inside the NCF, keeping in view of experimental ambiguity, has not been reported yet.

In this paper, we use numerical simulations to report the efficient channeling of single photons from a single quantum emitter into guided modes of the optical NCF. We perform numerical simulations to optimize the inner and outer diameters of the NCF filled with liquid medium by placing the SDS inside, which was not possible in the case of the ONF. A maximum η -value of 52% is found when the radially polarized SDS is placed at the center of the NCF filled with water medium. For the emission wavelength of 620 nm, the optimum inner and outer diameters of the NCF filled with water are 100 nm and 360 nm, respectively. Additionally, we investigate the position dependence of the SDS inside the NCF keeping in view of experimental ambiguity. Simulated results show that the η -value remains almost the same for the water medium while changing the position of the SDS inside the NCF.

2 Methodology

We perform numerical simulations using Ansys lumeral finite difference time domain (Ansys, FDTD Package) platform [30, 31]. First, we perform simulations to determine the η -value into guided modes of the ONF in vacuum and liquid medium for reference. Conceptual sketches of the ideas are shown in Figs. 1 (a) and (b) for vacuum and liquid medium, respectively. We determine the η -value for different diameters of the ONF (D_v/D_l) in both mediums. The SDS is placed on the surface of the ONF. We set the polarization of the SDS to be radial/azimuthal/axial. We place the power monitor (M) sufficiently far from the SDS position to determine the coupled power (P_c). P and P_0 are the total power emitted by the SDS in the presence of the ONF and in the vacuum environment, respectively. Thus, the channeling efficiency is defined as $\eta = P_c/P$. We determine the η -value for different polarizations while sweeping the D_v/D_l -values of the ONF. For each case, we find the optimum D_v/D_l -values by maximizing the η -value into the guided mode of the ONF.

Next, we perform simulations to determine the η -value for the NCF based on the optimum ONF diameters (D_v/D_l). Conceptual sketches of the NCF-filled with vacuum and liquid medium are shown in Figs. 2 (a) and (b), respectively. The SDS is placed inside the NCF. We determine the η -value for different polarizations while

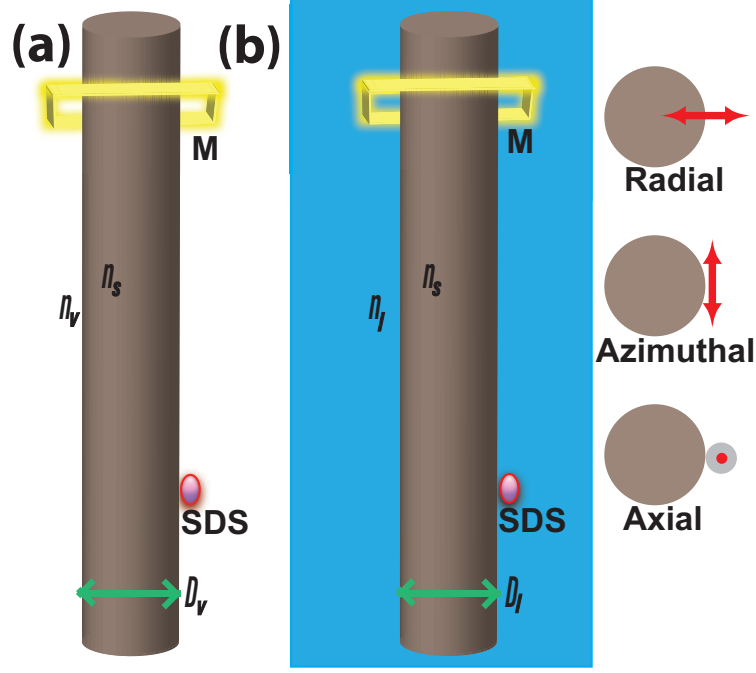


Fig. 1 (a) and (b) show the conceptual sketches of the ideas for the optical nanofiber (ONF) placed in vacuum and liquid medium, respectively. D_v and D_l are the ONF diameters when the surrounding medium is vacuum and liquid, respectively. n_s , n_v , and n_l are refractive indices of silica, vacuum, and liquid, respectively. SDS and M denote the single dipole source and monitor, respectively. The SDS is placed on the surface of the ONF. The insets show the radial, azimuthal, and axial polarizations corresponding to the SDS directed perpendicular, tangent, and parallel to the cylindrical surface, respectively.

sweeping inner and outer diameters (d^{in} and d^{out}) of the NCF in both mediums. The vacuum and liquid-filled NCFs are defined as hollow-core NCF and liquid-core NCF, respectively. For each case, we find the optimum d^{in} and d^{out} -values by maximizing the η -value into the guided mode of the NCF.

ONF, NCF, SDS, and M are placed inside the three-dimensional simulation area of $6 \times 6 \times 35 \mu m^3$ enclosed in the perfectly matched layers (PMLs) to avoid reflections. The length of the ONF/NCF is set at $45 \mu m$ so that they can be treated as infinitely long. The maximum ONF/NCF diameter is chosen within the simulation region. The SDS is placed $5 \mu m$ away from the PML. The M is placed $25 \mu m$ away from the SDS and $5 \mu m$ away from the PML. In the case of the ONF, the radial, azimuthal, and axial polarizations corresponding to the SDS are directed perpendicular, tangent, and parallel to the cylindrical surface, respectively as clearly shown in the inset of Fig. 1 (b). In the case of the NCF, the radial and axial polarizations corresponding to the SDS are directed perpendicular and parallel to the cylinder axis, respectively as clearly shown in the insets of Fig. 2. We set the emission wavelength of the SDS at 620 nm, corresponding to the emission wavelength of the quantum emitter [32]. In the case of the ONF, refractive indices of a cylinder and surrounding mediums are set for silica

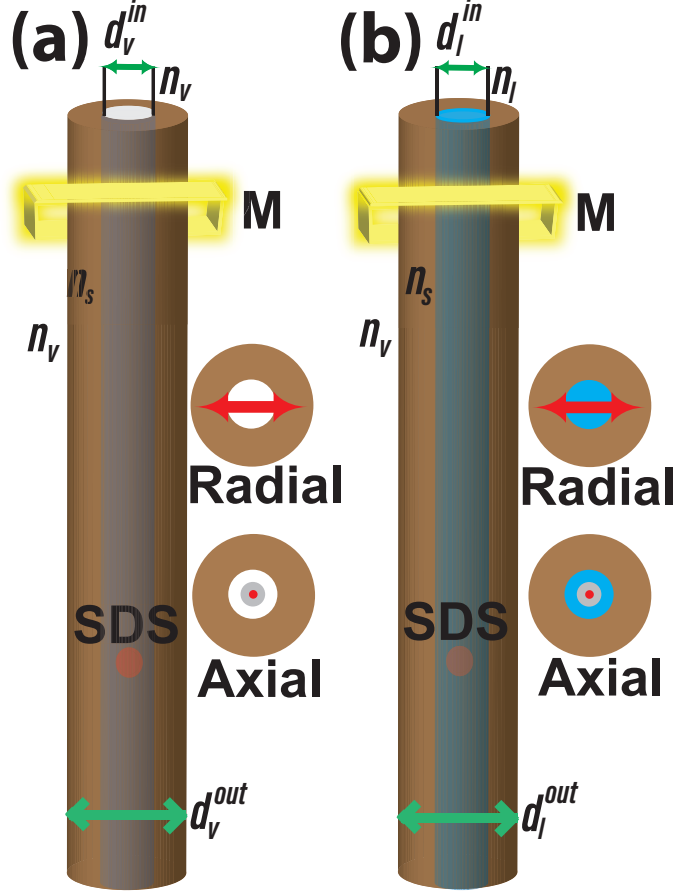


Fig. 2 (a) and (b) show the conceptual sketches of the ideas for the nanocapillary fiber (NCF) filled with vacuum and liquid medium, respectively. d_v^{in}/d_l^{in} and d_v^{out}/d_l^{out} are the inner and outer diameters of the NCF filled with vacuum/liquid, respectively. n_s , n_v , and n_l are refractive indices of silica, vacuum, and liquid, respectively. SDS and M denote the single dipole source and monitor, respectively. The SDS is placed inside the NCF. The insets show radial and axial polarizations corresponding to the SDS directed perpendicular and parallel to the cylinder axis, respectively.

(n_s) and vacuum (n_v)/liquid (n_l), respectively. In the case of the hollow core NCF, refractive indices of the outside of the cylinder, cylinder, and inside of the cylinder are set for vacuum (n_v), silica (n_s), and vacuum (n_v), respectively. In the case of the liquid core NCF, refractive indices of the outside of the cylinder, cylinder, and inside of the cylinder are set for vacuum (n_v), silica (n_s), and liquid (n_l), respectively.

3 Results

Figure 3 (a) shows the dependence of η -value as a function of the ONF diameter (D_v) for the SDS placed on the surface of the ONF. Horizontal and vertical axes correspond to the D_v -value and η -value, respectively. The SDS along the radial, azimuthal, and

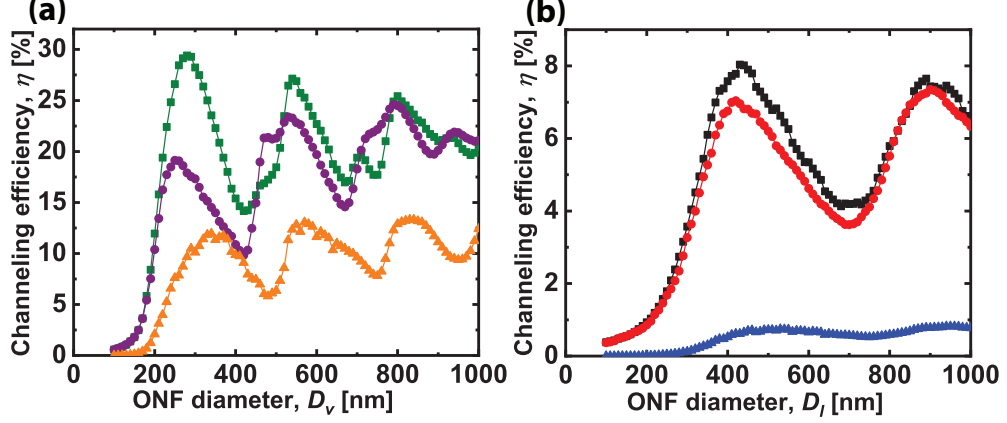


Fig. 3 (a) and (b) show summaries of η -values as a function of the optical nanofiber (ONF) diameters (D_v/D_l) for three polarizations when the ONF is placed in vacuum and water, respectively. Green/black squares, purple/red circles, and orange/blue triangles correspond to the radial, azimuthal, and axial polarizations, respectively.

axial polarizations are shown by green squares, purple circles, and orange triangles, respectively. One can readily see the maximum η -value is for the radial polarization. This is due to the strong confinement of the field in the radial direction. For the radial, azimuthal, and axial polarizations, we found the maximum η -value of 29%, 18%, and 9%, respectively. The maximum η -value of 29% occurred at the D_v -value of 280 nm, corresponding to the fiber size parameter of 1.42.

Figure 3 (b) shows the dependence of η -value as a function of the ONF diameter (D_l) for the SDS placed on the surface of the ONF and the surrounding medium is water. Horizontal and vertical axes correspond to D_l -value and η -value, respectively. The SDS along the radial, azimuthal, and axial polarizations are shown by black squares, red circles, and blue triangles, respectively. One can see that the maximum η -value occurred for the radial polarization. For the radial, azimuthal, and axial polarizations, we found the maximum η -value of 8%, 7%, and 1%, respectively. The maximum η -value of 8% occurred at the D_l -value of 430 nm, corresponding to the fiber size parameter of 2.17.

We perform simulations to determine the η -value for the NCF outer diameter based on the optimum η -value of ONF diameters in free space and water medium. The NCF outer diameter is chosen as the average value of optimum diameters of ONF in both free space and water medium. Then, we sweep the inner diameters while the outer diameter is fixed at the average value. Then, we fix the inner diameter of the NCF at the value where there is no significant decay in the η -value and consider the experimental realization of such a thin capillary hole. Then, we sweep the outer diameter of the NCF and find the optimum outer diameter of the NCF.

Figure 4 (a) shows the dependence of η -value as a function of the NCF inner diameters (d^{in}) filled with vacuum/water. Note that the SDS is placed at the center of the NCF. The outer diameter (d^{out}) of the NCF is fixed at 360 nm. Based on the previous simulation results, The d^{out} -value is chosen as the average value of optimum

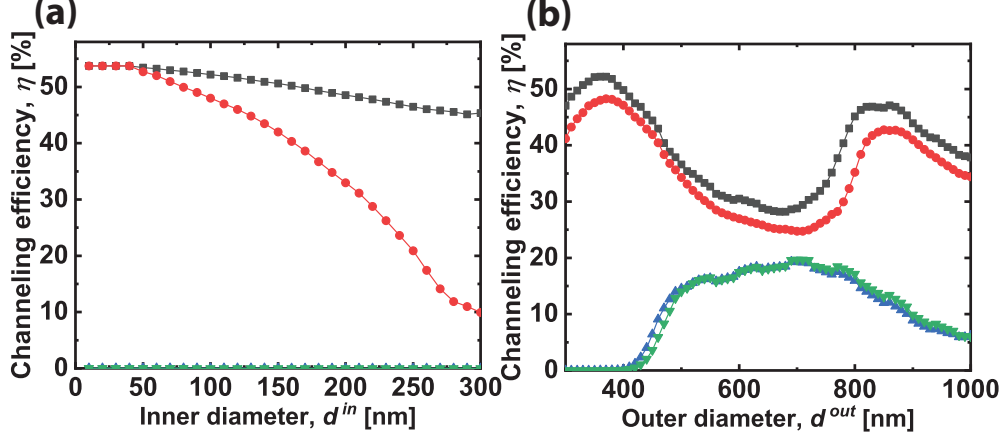


Fig. 4 (a) The summary of η -values as a function of the inner diameter (d^{in}) of the nanocapillary fiber (NCF) filled with vacuum and water for two polarizations. The outer diameter (d^{out}) of the NCF is fixed at 360 nm. (b) The summary of η -values as a function of d^{out} -values of the NCF filled with vacuum and water for two polarizations. The d^{in} -value of NCF is fixed at 100 nm. Black squares and red circles denote the radial polarization in water and vacuum, respectively. Blue and green triangles denote the axial polarization in water and vacuum, respectively.

D_v and D_l -values. The d^{in} -value of the NCF varies from 10 nm to 300 nm. The vertical axis corresponds to the η -value. Black squares and red circles represent the radial polarization of the SDS in water and vacuum, respectively. Blue and green triangles represent the axial polarization of the SDS in water and vacuum, respectively. In both cases, one can readily see that the maximum value occurred for the radial polarization. For the radial polarization, one can readily see that the maximum value occurred for the water medium. We found the maximum η -value of 53%. Note that the η -value for the radial and azimuthal polarizations are the same when the SDS is at the center of the NCF.

Figure 4 (b) shows the dependence of η -value as a function of the NCF outer diameter (d^{out}). The d^{in} -value of the NCF is fixed at 100 nm considering the experimental feasibility. The d^{out} -value of the NCF is varied from 300 nm to 1000 nm. The vertical axis corresponds to the η -value. Black squares and red circles represent the radial polarization in water and vacuum, respectively. Blue and green triangles represent the axial polarization in water and vacuum, respectively. One can readily see the maximum η -value occurred for the radial polarization. We found the maximum η -value of 52% at d^{out} -value of 360 nm corresponding to the fiber size parameter of 1.82. In the case of vacuum, the maximum η -value of 48% was found at d^{out} -value of 370 nm corresponding to the fiber size parameter of 1.87.

Considering experimental feasibility, we investigate the choice of d^{in} -value. Figure 5 (a) shows the dependence of η -value as a function of the outer diameter (d^{out}) of the NCF. The d^{in} -value of the NCF is fixed at 250 nm. The d^{out} -value of the NCF varies from 300 nm to 1000 nm. The vertical axis corresponds to the η -value. Black squares and red circles represent the radial polarization in water and vacuum, respectively. Blue and green triangles represent the axial polarization in water and

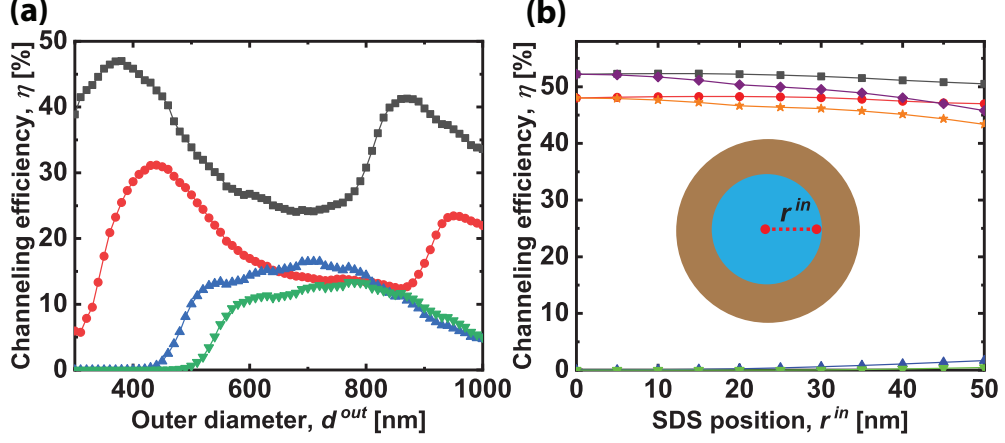


Fig. 5 (a) The summary of η -values as a function of outer diameter (d^{out}) of the nanocapillary fiber (NCF) filled with vacuum and water for two polarizations. The inner diameter (d^{in}) of the NCF is fixed at 250 nm. Black squares and red circles denote the radial polarization in water and vacuum, respectively. Blue and green triangles denote the axial polarization in water and vacuum, respectively. (b) The dependence of η -value as a function of the position (r^{in}) of the single dipole source (SDS) for three polarizations. The inner and outer diameters of the NCF are fixed at 100 nm and 360 nm, respectively. Black squares, purple diamonds, and blue triangles are for the radial, azimuthal, and axial polarizations in the water medium, respectively. Red circles, orange stars, and green triangles are for the radial, azimuthal, and axial polarizations in the vacuum, respectively. The inset shows the schematic for the position of the SDS.

vacuum, respectively. One can readily see the maximum η -value occurred for the radial polarization. We found the maximum η -value of 47% at the d^{out} -value of 380 nm corresponding to the fiber size parameter of 1.92. In the case of vacuum, the maximum η -value of 31% was found at the d^{out} -value of 440 nm corresponding to the fiber size parameter of 2.23.

Also, we investigate the effect of the position (r^{in}) of the SDS inside the NCF by considering the experimental ambiguity in placing a single quantum emitter. Figure 5 (b) shows the dependence of η -value as a function of r^{in} -value. The d^{in} and d^{out} -values of the NCF are kept constant at 100 nm and 360 nm, respectively. The horizontal axis corresponds to the r^{in} -value, which varies from 0 nm (center) to 50 nm (inside edge) as shown in the inset of Fig. 5 (b). The vertical axis corresponds to the η -value. Black squares, purple diamonds, and blue triangles are for the radial, azimuthal, and axial polarizations in the water medium, respectively. Red circles, orange stars, and green triangles are for the radial, azimuthal, and axial polarizations in the vacuum, respectively. In both cases, one can readily see that the η -value corresponding to the radial polarization is maximum. Note that in both cases of the axial polarization, the η -value is close to 1%.

4 Discussion

The single-mode condition is defined by the parameter $V = ka\sqrt{n_1^2 - n_2^2} < 2.405$, where a is the ONF radius, $k = 2\pi/\lambda$, λ is wavelength of the light, and n_1 and n_2 are refractive

indices of the core and clad, respectively [14, 33, 34]. To satisfy the single-mode condition for the emission wavelength of 620 nm, the maximum ONF diameters (D_v/D_l) are 450 nm and 820 nm for the clad medium of vacuum and water, respectively. The maximum D_v and D_l -values for single mode condition differ significantly. This is due to the significant difference in the refractive index between the silica and vacuum compared to silica and water. As seen clearly in Figs. 3 (a) and (b), that multimode behavior appears at the expected ONF diameters, resulting in increasing the η -value for the thicker diameter of the ONF.

As seen in Figs. 3 (a) and (b), the optimum ONF diameters in a single-mode regime differ for three polarizations. The optimum D_v/D_l -values are 250/420 nm, 280/430 nm, and 340/460 nm for azimuthal, radial, and axial polarizations, respectively. This is due to the effective refractive index difference in three different polarizations. In Fig. 3 (a), the maximum η -value of 29% is found for the radial polarization, which is in good agreement with the previously reported works in Refs. [18, 19]. The average η -value is 20%, assuming the randomly oriented dipoles, which is in good agreement with the experimentally reported η -value in Ref. [16]. In Fig. 3 (b), the maximum η -value of 8% is found for the radial polarization. The average η -value is 5%, considering the randomly oriented dipoles for the experimental feasibility. The difference in the maximum η -value is due to the weak field confinement around the ONF. However, the ONF in water medium will find various applications for bio-sensing [35].

As seen in Figs. 4 (a) and (b), one can readily see the maximum and minimum η -values are for the radial and axial polarizations for both mediums, respectively. This is due to the axial component (E_z) of the electric field being low at the center of the NCF as discussed in Ref. [33]. In Fig. 4 (a), the maximum η -value for the radial polarization is almost the same for water and vacuum mediums up to d^{in} -value of 40 nm. However, a significant change for η -value occurred for the d^{in} -value from 50 nm to 300 nm for the vacuum compared to the water medium. This is due to the significant change in the effective refractive index of the NCF while the d^{in} -value is high. In contrast, as seen in Fig. 4 (b), one can readily see that as d^{out} -value increases the η -value for axial polarization increases. This may be due to the coupling to multi-modes (higher-order).

For the radial polarization, a maximum η -value of 52% is realized at d^{in} -value of 100 nm and d^{out} -value of 360 nm of the NCF. In contrast, as seen in Fig. 5 (a), one can readily see the maximum η -value for the radial and axial polarizations get affected when the d^{in} is fixed at 250 nm. For the radial polarization, a maximum η -value of 47% is realized at the d^{in} -value of 250 nm and the d^{out} -value of 380 nm of the NCF. This is due to the weak field confinement inside the NCF because of the effective refractive index change as the inner diameter increases. We also simulated η -value for the azimuthal polarization and found the same result as the radial polarization. This is due to the placement of the SDS at the center in contrast to the SDS on the surface of the ONF. Note that η -value of 52% is almost two times the values compared to the SDS placed on the surface of the ONF [18, 19]. The present value is almost 1.4 times the value compared to the SDS placed on the facet of the ONFT. Compared to other existing fiber-based platforms, the NCF is a promising avenue. The average η -value is 35%, assuming the randomly oriented dipoles, which is higher than the experimentally reported η -value for the ONF in Ref. [16].

Two key challenges are to be achieved regarding the experimental feasibility of the present simulations. One is the fabrication of the NCF with such a small capillary hole and the other is placing a single quantum emitter inside the NCF. Commercial capillary optical fibers can be tapered to sub-wavelength diameters to realize NCF using a heat and pull technique [14, 36, 37]. The placement of a single quantum emitter inside the NCF can be achieved by flowing through the center of the NCF by pushing the liquid from one end of the NCF. Considering the experimental realization of the simulation results, we choose water medium as quantum dots are dissolved in water. Regarding the sensitivity of the inner and outer diameters of the NCF to the η -value, one can readily see in Figs. 4 and Fig. 5 (a) that the peak η -values occurred in rather broad, not sharp. This implies that if there is any slight ambiguity in the inner and outer diameters of the NCF, it doesn't affect the η -value significantly. This would give additional freedom in the experimental realization.

As seen in Fig. 5 (b), the η -value is almost unchanged while changing the r^{in} -value for the radial polarization. This suggests that the SDS position inside the NCF is not necessarily at the center to realize the maximum interaction i.e. maximum η -value. This would enable the easy experiments to place a single quantum emitter inside the NCF, as it is challenging to control the position of a single quantum emitter inside the NCF. Note that no significant change occurs for azimuthal polarization while changing the r^{in} -values up to 50 nm. In any case, the maximum η -value of more than 50% can be realized using the NCF.

The η -value can be further enhanced in two possible ways: one is creating a cavity structure on the NCF [28, 38–40], and the other is increasing the refractive index of the medium and material. Regarding cavity, simulations suggest that η -value can be as high as 80%, which is higher than the experimentally reported values of 65% if the ONF is replaced with the NCF. Regarding increasing refractive index, simulations suggest that η -value can be higher than the present value if the silica is replaced with other high refractive index material like diamond/silicon nitride/gallium phosphate [26]. Also, the refractive index of the medium can affect the η -value if we replace water with any higher refractive index liquid [29].

5 Conclusion

In summary, we reported numerically the efficient channeling of single photons from a single quantum emitter into guided modes of NCFs. The maximum channeling efficiency of 52% is found when the radially polarized dipole is placed at the center of the NCF in the liquid (water) medium. The optimum inner and outer diameters of the NCF are 100 nm and 360 nm, respectively for the emission wavelength of 620 nm. Additionally, we investigated the SDS position dependence inside the NCF considering experimental discrepancies in placing the single quantum emitter inside the NCF. We found that the channeling efficiency remains almost the same for the water medium at the optimum condition. The present platform may open a novel route for quantum technologies and bio-sensing.

Acknowledgments. RRY acknowledges financial support from the Scheme for Transformational and Advanced Research in Sciences (STARS) grant from the Indian

Institute of Science (IISc), Ministry of Human Resource Development (MHRD) (File No. STARS/APR2019/PS/271/FS) and the Institute of Eminence (IoE) grant at the University of Hyderabad, Ministry of Education (MoE) (File No. RC2-21-019). RM acknowledges the University Grants Commission (UGC) for the financial support (Ref. No.:1412/CSIR-UGC NET June 2019).

Author contributions. BE performed the numerical calculations and plotted the graphs. BE wrote the manuscript under the supervision of RRY. All authors reviewed the manuscript. This work forms a part of the PhD thesis of BE.

Declarations

Ethical Approval. Not applicable. No human and/or animal studies have been executed.

Funding. To prepare this manuscript, funding was received by Institute of Eminence (IoE) grant at the University of Hyderabad, Ministry of Education (MoE) (File No. RC2-21-019).

Availability of data and materials. Data underlying the results presented in this paper are not publicly available at this time but may be obtained from the authors upon reasonable request.

Conflict of interest. The authors declare no conflict interests.

Competing interests. The authors declare no competing interests.

References

- [1] Hood, C.J., Lynn, T., Doherty, A., Parkins, A., Kimble, H.: The atom-cavity microscope: Single atoms bound in orbit by single photons. *Science* **287**(5457), 1447–1453 (2000)
- [2] Barros, H., Stute, A., Northup, T., Russo, C., Schmidt, P., Blatt, R.: Deterministic single-photon source from a single ion. *New Journal of Physics* **11**(10), 103004 (2009)
- [3] Fleury, L., Segura, J.-M., Zumofen, G., Hecht, B., Wild, U.: Nonclassical photon statistics in single-molecule fluorescence at room temperature. *Physical review letters* **84**(6), 1148 (2000)
- [4] Michler, P., Imamoglu, A., Mason, M., Carson, P., Strouse, G., Buratto, S.: Quantum correlation among photons from a single quantum dot at room temperature. *Nature* **406**(6799), 968–970 (2000)
- [5] Kurtsiefer, C., Mayer, S., Zarda, P., Weinfurter, H.: Stable solid-state source of single photons. *Physical review letters* **85**(2), 290 (2000)

- [6] Aharonovich, I., Englund, D., Toth, M.: Solid-state single-photon emitters. *Nature photonics* **10**(10), 631–641 (2016)
- [7] Kimble, H.J.: The quantum internet. *Nature* **453**(7198), 1023–1030 (2008)
- [8] Bremer, L., Rodt, S., Reitzenstein, S.: Fiber-coupled quantum light sources based on solid-state quantum emitters. *Materials for Quantum Technology* (2022)
- [9] Solomon, G., Pelton, M., Yamamoto, Y.: Single-mode spontaneous emission from a single quantum dot in a three-dimensional microcavity. *Physical Review Letters* **86**(17), 3903 (2001)
- [10] Schröder, T., Gädeke, F., Banholzer, M.J., Benson, O.: Ultrabright and efficient single-photon generation based on nitrogen-vacancy centres in nanodiamonds on a solid immersion lens. *New Journal of Physics* **13**(5), 055017 (2011)
- [11] Shambat, G., Provine, J., Rivoire, K., Sarmiento, T., Harris, J., Vučković, J.: Optical fiber tips functionalized with semiconductor photonic crystal cavities. *Applied Physics Letters* **99**(19), 191102 (2011)
- [12] Patel, R.N., Schröder, T., Wan, N., Li, L., Mouradian, S.L., Chen, E.H., Englund, D.R.: Efficient photon coupling from a diamond nitrogen vacancy center by integration with silica fiber. *Light: Science & Applications* **5**(2), 16032–16032 (2016)
- [13] Akimov, A., Mukherjee, A., Yu, C., Chang, D., Zibrov, A., Hemmer, P., Park, H., Lukin, M.: Generation of single optical plasmons in metallic nanowires coupled to quantum dots. *Nature* **450**(7168), 402–406 (2007)
- [14] Nayak, K.P., Sadgrove, M., Yalla, R., Le Kien, F., Hakuta, K.: Nanofiber quantum photonics. *Journal of Optics* **20**(7), 073001 (2018)
- [15] Vetsch, E., Reitz, D., Sagué, G., Schmidt, R., Dawkins, S., Rauschenbeutel, A.: Optical interface created by laser-cooled atoms trapped in the evanescent field surrounding an optical nanofiber. *Physical review letters* **104**(20), 203603 (2010)
- [16] Yalla, R., Le Kien, F., Morinaga, M., Hakuta, K.: Efficient channeling of fluorescence photons from single quantum dots into guided modes of optical nanofiber. *Physical review letters* **109**(6), 063602 (2012)
- [17] Fujiwara, M., Toubaru, K., Noda, T., Zhao, H.-Q., Takeuchi, S.: Highly efficient coupling of photons from nanoemitters into single-mode optical fibers. *Nano letters* **11**(10), 4362–4365 (2011)
- [18] Le Kien, F., Gupta, S.D., Balykin, V., Hakuta, K.: Spontaneous emission of a cesium atom near a nanofiber: Efficient coupling of light to guided modes. *Physical Review A* **72**(3), 032509 (2005)

- [19] Klimov, V.V., Ducloy, M.: Spontaneous emission rate of an excited atom placed near a nanofiber. *Physical Review A* **69**(1), 013812 (2004)
- [20] Chonan, S., Kato, S., Aoki, T.: Efficient single-mode photon-coupling device utilizing a nanofiber tip. *Scientific reports* **4**(1), 4785 (2014)
- [21] Yonezu, Y., Wakui, K., Furusawa, K., Takeoka, M., Semba, K., Aoki, T.: Efficient single-photon coupling from a nitrogen-vacancy center embedded in a diamond nanowire utilizing an optical nanofiber. *Scientific reports* **7**(1), 12985 (2017)
- [22] Morrissey, M.J., Deasy, K., Frawley, M., Kumar, R., Prel, E., Russell, L., Truong, V.G., Chormaic, S.N.: Spectroscopy, manipulation and trapping of neutral atoms, molecules, and other particles using optical nanofibers: a review. *Sensors* **13**(8), 10449–10481 (2013)
- [23] Yang, L., Zhou, Z., Wu, H., Dang, H., Yang, Y., Gao, J., Guo, X., Wang, P., Tong, L.: Generating a sub-nanometer-confined optical field in a nanoslit waveguiding mode. *Advanced Photonics* **5**(4), 046003–046003 (2023)
- [24] Yalla, R., Kojima, Y., Fukumoto, Y., Suzuki, H., Ariyada, O., Shafi, K.M., Nayak, K.P., Hakuta, K.: Integration of silicon-vacancy centers in nanodiamonds with an optical nanofiber. *Applied Physics Letters* **120**(24) (2022)
- [25] Resmi, M., Bashaiah, E., Das, B., Yalla, R.: Efficient fiber-coupled single photon source using an optical nanofiber tip. In: *Women in Optics and Photonics in India 2022*, vol. 12638, pp. 107–109 (2023). SPIE
- [26] Das, B., Resmi, M., Bashaiah, E., Yalla, R.: Efficient single-mode coupling design using a silica/diamond nano-tip with a gold nanoparticle. In: *Women in Optics and Photonics in India 2022*, vol. 12638, pp. 125–127 (2023). SPIE
- [27] Resmi, M., Elaganuru, B., Ramachandrarao, Y.: Channeling of fluorescence photons from quantum dots into guided modes of an optical nanofiber tip. *arXiv* **2401.16891** (2024)
- [28] Yalla, R., Sadgrove, M., Nayak, K.P., Hakuta, K.: Cavity quantum electrodynamics on a nanofiber using a composite photonic crystal cavity. *Physical review letters* **113**(14), 143601 (2014)
- [29] Faez, S., Türschmann, P., Haakh, H.R., Götzinger, S., Sandoghdar, V.: Coherent interaction of light and single molecules in a dielectric nanoguide. *Physical review letters* **113**(21), 213601 (2014)
- [30] Taflov, A., Hagness, S.C., Picket-May, M.: Computational electromagnetics: the finite-difference time-domain method. *The Electrical Engineering Handbook* **3**(629-670), 15 (2005)

- [31] Schneider, J.B.: Understanding the finite-difference time-domain method. School of electrical engineering and computer science Washington State University **28** (2010)
- [32] Shafi, K.M., Luo, W., Yalla, R., Iida, K., Tsutsumi, E., Miyanaga, A., Hakuta, K.: Hybrid system of an optical nanofibre and a single quantum dot operated at cryogenic temperatures. Scientific reports **8**(1), 13494 (2018)
- [33] Le Kien, F., Liang, J., Hakuta, K., Balykin, V.: Field intensity distributions and polarization orientations in a vacuum-clad subwavelength-diameter optical fiber. Optics Communications **242**(4-6), 445–455 (2004)
- [34] Okamoto, K.: Fundamentals of Optical Waveguides. Elsevier, ??? (2021)
- [35] Mauranyapin, N., Madsen, L., Taylor, M., Waleed, M., Bowen, W.: Evanescent single-molecule biosensing with quantum-limited precision. Nature Photonics **11**(8), 477–481 (2017)
- [36] Ward, J.M., O’Shea, D.G., Shortt, B.J., Morrissey, M.J., Deasy, K., Nic Chormaic, S.G.: Heat-and-pull rig for fiber taper fabrication. Review of scientific instruments **77**(8) (2006)
- [37] Tong, L., Gattass, R.R., Ashcom, J.B., He, S., Lou, J., Shen, M., Maxwell, I., Mazur, E.: Subwavelength-diameter silica wires for low-loss optical wave guiding. Nature **426**(6968), 816–819 (2003)
- [38] Yalla, R., Muhammed Shafi, K., Nayak, K.P., Hakuta, K.: One-sided composite cavity on an optical nanofiber for cavity qed. Applied Physics Letters **120**(7) (2022)
- [39] Yalla, R., Hakuta, K.: Design and implementation of a tunable composite photonic crystal cavity on an optical nanofiber. Applied Physics B **126**(11), 187 (2020)
- [40] Li, W., Du, J., Truong, V.G., Nic Chormaic, S.: Optical nanofiber-based cavity induced by periodic air-nanohole arrays. Applied Physics Letters **110**(25) (2017)